J. Min. Metall. Sect. B-Metall. 55 (2) B (2019) 283 - 293

Journal of Mining and Metallurgy, Section B: Metallurgy

INFLUENCE OF NICKEL ADDITION AND CASTING MODULUS ON THE PROPERTIES OF HYPO-EUTECTIC DUCTILE CAST IRON

E. Colin-García [a], A. Cruz-Ramírez [a*], G. Reyes-Castellanos [a], J.A. Romero-Serrano [a], R.G. Sánchez-Alvarado [a], M. Hernández-Chávez [b]

[a*] Instituto Politécnico Nacional – ESIQIE, Departamento de Ingeniería en Metalurgia y Materiales, Ciudad de México, México

[b] Instituto Politécnico Nacional – UPIIH, Departamento de Formación Básica Disciplinaria, Pachuca, México

(Received 12 October 2018; accepted 19 March 2019)

Abstract

The effect of the casting modulus on the distribution and features of graphite in hypo-eutectic ductile iron unalloyed and alloyed with nickel (0.88 wt %) was studied. The cooling rate of the casting plates of 25.4, 12.7 and 8.5 mm in thickness with a casting modulus of 6.87, 4.46 and 3.31 mm, respectively promotes several microstructural changes, such as cementite precipitation and a noticeable nodule count increment. The nickel addition suppressed the cementite formation and improved the nodule count and nodularity for the three casting modulus evaluated. The nickel addition increased the nodule count in 69, 67 and 128 % for the modulus of 3.31, 4.46 and 6.87 mm, respectively, regarding the unalloyed ductile iron. It was found that the biggest casting modulus produced the biggest nodules with the lowest nodule count for both ductile cast irons. Further to the improvements in the graphite features, the nickel addition allowed to keep almost constant the yield and tensile strength ratio for the different casting modulus.

Keywords: *Ductile iron; Nodule count; Nickel; Casting modulus; Mechanical properties*

1. Introduction

Ductile cast iron is a casting material that has been most dynamic in winning new areas of application in recent years, due to its outstanding mechanical properties and moderate cost. The structure and properties of ductile cast iron are obtained in a foundry as a result of a melting process. In general, they depend on the chemical composition of the melt, physical state of the liquid iron, as well as on the cooling rate of the casting [1, 2]. Ductile iron is an iron-based alloy which contains a carbon content that is high enough to exceed its solubility in iron, resulting in the presence of pure carbon or graphite dispersed within an iron matrix. In the case of ductile iron, the shape of the graphite is spheroidal or round and is described as having graphite nodules. In the case of chemical composition control, some alloying elements are essential to play an important role in influencing the microstructure of ductile iron besides the major elements of carbon and silicon. A close control must be maintained over elements such as cerium, calcium, aluminum, and zirconium, which are known to promote graphite precipitates. Other elements, which favor the formation of pearlite and /or iron carbides, such as copper, chromium, and vanadium, must also be carefully controlled to avoid the detrimental effect on ductility [3-5]. Also, it is well known that nickel is a most commonly used alloying element because it decreases primary carbide stability while increasing the finesses of pearlite, thus increasing the strength of the iron [5]. High-nickel ductile iron has been specified by the ASTM A439 standard for its resistance to heat and corrosion as well as for other special purposes [6]. The properties of ductile iron are largely dependent on the relative amounts of ferrite and pearlite present within the matrix microstructure. Microstructure has to do with the alloying elements. Many of these elements define the matrix microstructure and mechanical properties. Matrix microstructure in some way influences the hardness of the cast [7]. R. Gonzaga and J. Carrasquilla [8] determined the influence of the alloying elements on microstructure and mechanical properties of ductile cast iron. They found that the right balance of each alloying element, the microstructure of the matrix, as well as the mechanical properties of the casting can be predicted. The number and shape of the graphite nodules are important when producing ductile iron. These

**Corresponding author: alcruzr@ipn.mx*

DOI:10.2298/JMMB181012023C

characteristics are described as the nodule count and nodularity, respectively [9]. Ductile cast iron is an important construction material within the cast iron family. The production of heavy section ductile iron castings is increasing and future applications seem to require even larger wall-thicknesses; however, several different graphite morphologies have been observed to form in the thermal center of heavy ductile iron sections during slow solidification [10]. On the other hand, the development of ductile iron has introduced thin-walled ductile iron as an improvement, in order to increase the strength to weight ratio and, in consequence, its competitiveness against light alloys. The high cooling rate taking place during solidification of thin wall ductile iron castings promotes two main changes in the microstructure: a) the precipitation of iron carbides and b) an important increase in the nodule count. It has been reported [11, 12] that thin walls with less than 4 mm thickness increase the nodule count up to 2000 nod mm^{-2}. The literature shows that a moderate increase in nodule count in normal wall parts from 100 to 150 nod mm^{-2}, increases the strength and ductility, due to a finer and more homogeneous microstructure obtained by austempering [13]. The resulting finer microstructure decreases the distance for carbon diffusion and increases the number of graphite matrix interfaces [14]. It has been reported [15, 16] that an increase in the nodule count promotes an increase in the resistance to abrasive wear rate and rolling contact fatigue wear. Ductile irons selected to cast thin walled parts are commonly unalloyed and the resulting matrix is more homogeneous than that of alloyed ductile iron [17]. The matrix homogeneity is also favored by rapid solidification since last to freeze regions are smaller and more dispersed; however, the large supercooling caused by the higher cooling rate may induce the solidification to proceed totally or partially leading to the precipitation of cementite. The main cause of the undesirable cementite formation tendency in thin wall castings is due to the low carbon equivalent of the casting [18]. The casting modulus is used to determine in a simple way the relative solidification times of casting sections and risers [19]. The volume-to-area ratio of the casting is termed the casting modulus. Therefore, modulus more accurately represents the heating and cooling properties of the casting. Since not many published research articles are available on the nickel effect on the microstructure and mechanical properties of ductile cast iron [20], the present work aims at the study of the influence of casting sections of 8.5, 12.7 and 25.4 mm based on the casting modulus on the microstructure and mechanical properties of hypo-eutectic ductile irons, unalloyed and alloyed with 0.88 wt. % nickel in the as-cast condition.

2. Materials and Experimental procedures

A pattern including six plates of 120 x 40 mm with a thickness ranging from 25.4 to 4.23 mm was designed to enable investigation of the influence of different thickness on nodule count and microstructure formation (Figure 1).

Two melts, identified as A for the unalloyed ductile iron and B for the ductile alloyed with 0.88 wt % Ni, were produced in a 50 Kg medium-frequency coreless induction furnace and cast in green sand molds. The base iron was prepared with a mixture of 35 wt % low C and Mn steel, 35 wt % pig iron and 35% cast iron scrap as the metallic charge. High purity carbon riser, FeSi (75 %) and high purity Ni (99 %) were used to adjust the chemical composition of the charge. The base iron was inoculated by 1.0 % foundry grade FeSi (75% Si+ 1%Ca, 0.9% Al, 1.1% Ba) in pouring ladle and then, treated by 1.5 % nodulizing MgFeSi (45 %Si, 8% Mg, 3.3%Ca, 3% Rare Earths) alloy in transfer ladle using sandwich process. The nominal chemical composition analyzed in the castings was analyzed by an Oxford spark emission optic spectrograph and the reported values in Table 1 are the average of five measurements on each heat.

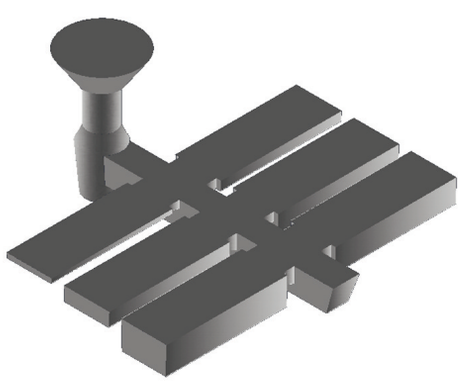

Figure 1. *Pattern plate model including six plates of 120 x 40 mm with a thickness ranging from 25.4 to 4.23 mm*

Table 1. *Chemical composition (wt. %) of the heats*

Heat	C	Si	Mn	P	S	Mg	Ni	Cr	Mo	Al	Cu	V	Sn	CE
A	3.21	2.84	0.18	0.02	0.02	0.04	0.01	0.10	<0.005	0.02	0.06	0.01	0.04	4.17
B	3.11	2.72	0.16	0.02	0.01	0.06	0.88	0.10	<0.005	0.02	0.07	0.01	0.05	4.02

CE: Carbon equivalent. Balance Fe

The use of casting modulus (casting cooling rate) rather than casting section was used to describe more accurately the cooling rate. The plates of 25.4, 12.7 and 8.5 mm in thickness with a casting modulus of 6.87, 4.46 and 3.31 mm, respectively were characterized by optical microscopy, scanning electron microscopy (SEM) with energy dispersive spectra (EDS), x-ray diffraction (XRD) and mechanical test. Standard metallography techniques (mechanical grinding and polishing followed by etching with 2 % nital) were employed to reveal the different micro-constituents of the structure. Optical microscopy was performed on polished and 2% nital etched specimens by using an optical microscope Olympus PMG-3 model, the ASTM A 247 standard and the image-analyzer with the software Image J 4.1 version. The graphite morphology was rated for the nodularity and nodule count in accordance with

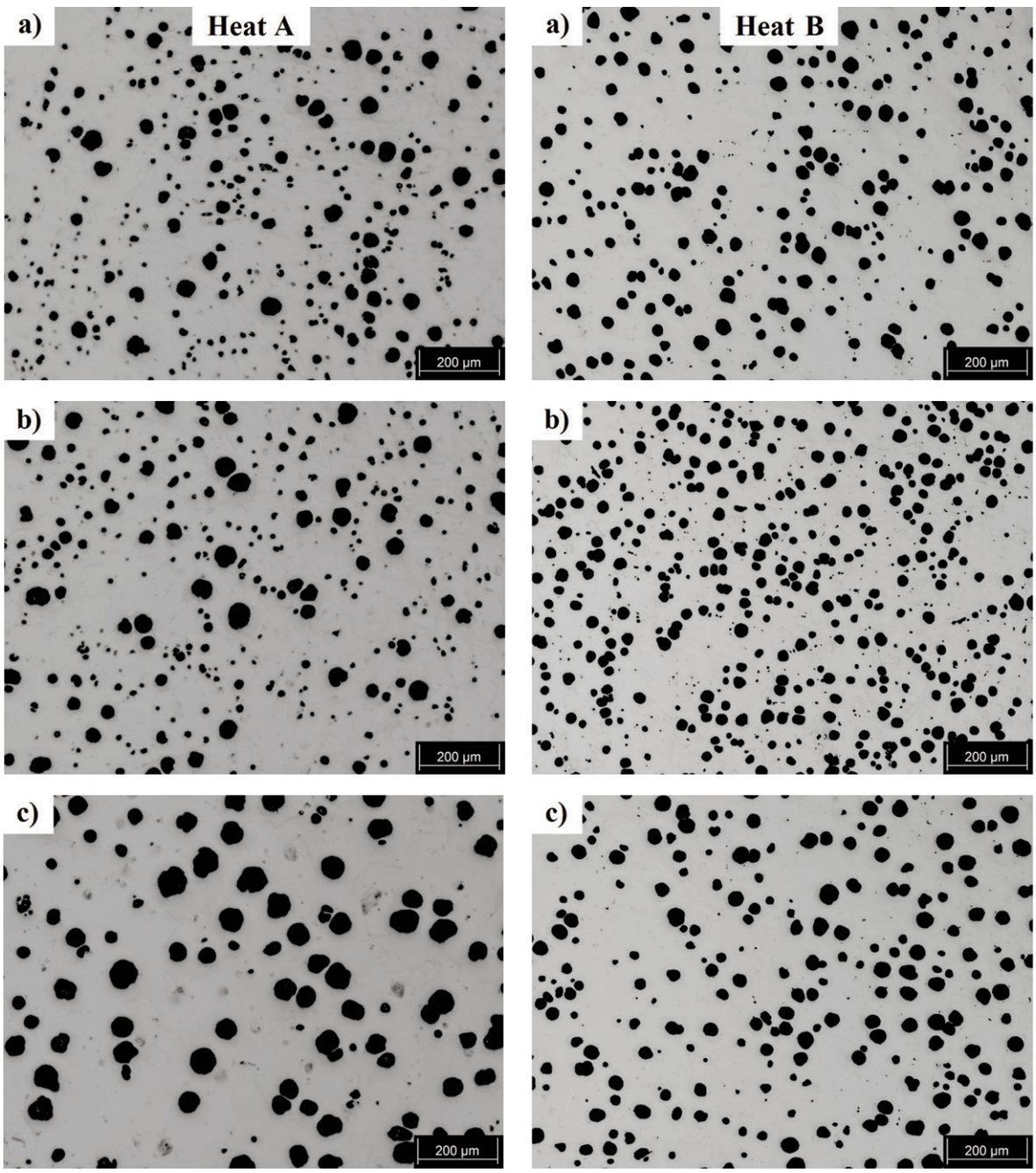

Figure 2. *Unetched microstructure of heats A and B for a casting modulus of a) 3.31 mm, b) 4.46 mm and c) 6.87 mm*

ASTM standard A 247 on the unetched samples. Phase volume fraction measurements including nodule graphite, pearlite, ferrite, and carbides were carried out using the image-analyzer with the software Image J 4.1. Carbides were revealed by etching 2 min with a water solution of ammonium persulfate (10% vol) [21]. The optical microscopy measurements represent the average of eight different regions on each sample.

The phases of the matrix were identified by X-ray diffraction measurements using an X-Ray Bruker D8 Focus with monochromatic Cu Kα radiation working in θ/2θ configuration. Data were collected in an angular range from 35 to 100° with a step size of 0.02° and a counting time of 2 °min^{-1}.

High definition images on the matrix were taken with a scanning electron microscope (SEM) JEOL model 6701 F. Images were obtained to different magnifications with backscattering electrons of 15 kV.

Samples of the ductile cast irons were obtained from the central region of the plates by machining in the longitudinal direction for tensile and Brinell hardness. The Brinell hardness measurements were carried out in the longitudinal direction using a Wilson durometer series 500 in accordance with the standard specification of ASTM E10. At least six measurements were taken from each sample and the average and standard deviation are reported. The size and geometry of the specimens were in accordance with specifications of ASTM E8 and ASTM E10 for the tension and hardness testing, respectively. Tensile testing was carried out at room temperature using a universal testing machine Shimadzu of 100 KN with 10 mm/min cross-head speed. Three specimens from each heat were tested for tensile tests and the average and standard deviation are reported.

3. Results and discussion

The nominal chemical composition analyzed in the castings are shown in Table 1. The chemical composition of the heats produced was similar, and the only difference was the amount of nickel added to the heat B. In both cases the equivalent carbon was hypo-eutectic. A high silicon content was used in order to improve graphitization under the high cooling rates imposed by the casting modulus. A residual magnesium content of 0.05% in average was obtained for an adequate nodule formation.

Figure 2 shows the unetched microstructure of heats A and B. A homogeneous distribution of spheroidal graphite for both heats with a high nodularity and nodule count is observed.

The nodularity, nodule count, and average nodule size values of heats in the as-cast condition are shown in Table 2 for the modulus evaluated. Figure 3 and 4 show the behavior of the nodule count and the average nodule size as a function of the casting modulus, respectively.

Figure 3 shows that for the case of heat A the values ranged from 127 nod mm^{-2}, for the 6.87 mm modulus, up to 357 nod mm^{-2} for the modulus of 3.31 mm. However, for the case of heat B, the nodule count was increased from 290 to 606 nod mm^{-2} when the modulus was decreased from 6.87 mm to 3.31 mm,

Table 2. *Distribution and features of graphite in the cast ductile iron*

Casting modulus (mm)	Heat A			Heat B		
	3.31	4.46	6.87	3.31	4.46	6.87
Nodularity (%)	85	83	80	88	90	89
Nodule count (nod mm^{-2})	357	312	127	606	523	290
Average nodule size (μm)	21.95	30.8	68.22	28.1	33.4	42.4

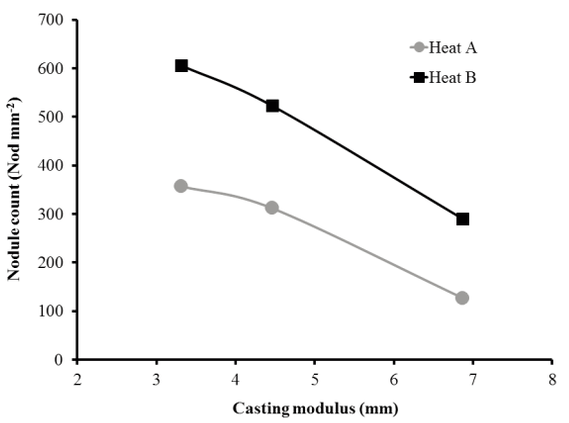

Figure 3. *Casting modulus effect on the nodule count for heats A and B*

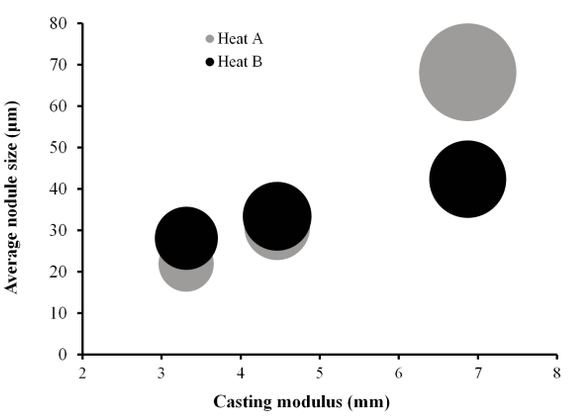

Figure 4. *Casting modulus effect on the nodule size average for heats A and B*

respectively. Similar behavior was reported in previous studies on the eutectic solidification of spheroidal graphite iron [11, 22]. Increasing the modulus (bigger section size) slows down the cooling rate, which results in a low nodule count. Increased nodule count is commonly followed by higher amounts of carbon and silicon and, at the same time, by the influence of magnesium. In our case, the carbon, silicon and magnesium contents were similar for both heats, with the only variation in the nickel content. This means that the nickel addition increases the nodule count in 69, 67 and 128 % for the modulus of 3.31, 4.46 and 6.87 mm, respectively, regarding the unalloyed ductile iron. The nodule count is especially important when alloy additions are made. Low nodule counts lead to larger spacing between the graphite nodules and larger regions of segregation, higher nodule counts will break up the segregated regions.

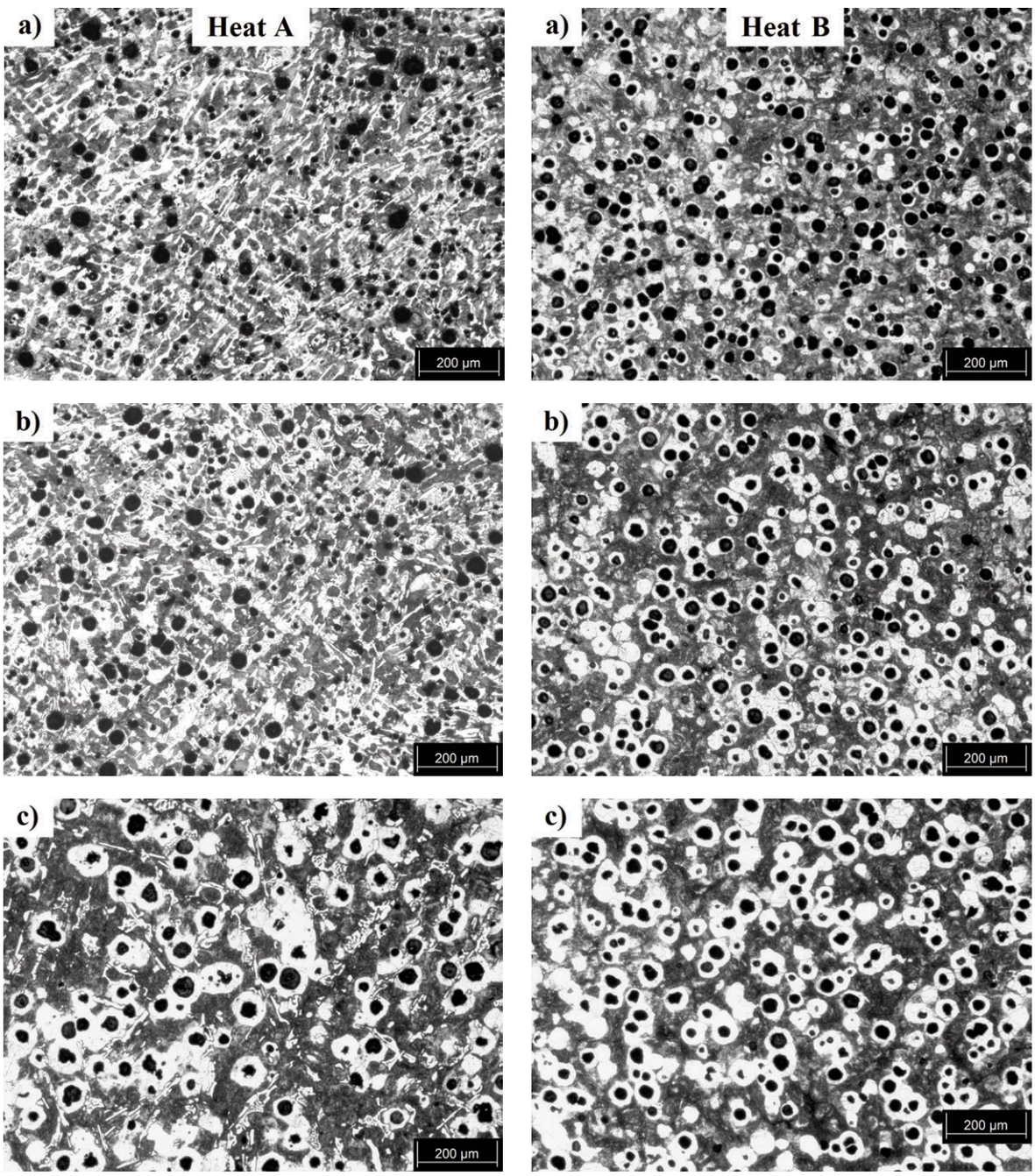

Figure 5. *Etched microstructure of heats A and B for a casting modulus of a) 3.31 mm, b) 4.46 mm and c) 6.87 mm*

In addition, P. Sellamuthu et al [20] studied the effect of adding 0.6, 0.8 and 1 wt. % Ni on the microstructure and mechanical properties of austempered ductile iron. The ductile iron samples were obtained from Y-blocks castings. They report that the nodule counts increased with the increase in the nickel content up to 0.8 wt. % and then dropped. Considering the measurements of the Y-block casting used, their casting modulus corresponds to 7.4, they report an average nodule count of 215 nod mm^{-2} for the nickel addition of 0.8 wt. %. This result fits with the trend of the nodule count reported in table 2 for heat B.

Figure 4 shows that the average nodule size was increased when the modulus was also increased for both heats. For heat B, an increase is observed in the average nodule size of 28 and 8.4% for the casting modulus of 3.31 and 4.46 mm, respectively, regarding heat A; however for the modulus of 6.87 mm, the average nodule size of heat B was decreased in 62% regarding heat A. It is observed clearly from Figure 4 that the increase of the average nodule size in heat B is slight and homogeneous, as the casting modulus is increased; however, for heat A, there is a remarkable increase in the average nodule size for the modulus of 6.87 mm regarding previous modulus. This behavior is also observed in the nodule count results in Figure 3, where the curve has a smooth trend for heat B, while the curve of heat A shows a discontinuous trend. There is a direct relation between the nodule count size and the average nodule size, it is shown that the biggest casting modulus produces the biggest nodules with the lowest nodule count for both heats. It has been reported for conventional ductile iron and austempered ductile iron [23, 24] that the nodule size is inversely proportional to the nodule count for both sand and metal mold ingots.

From Table 2, it is observed that the nickel addition improves the nodularity for the casting modulus evaluated. The percentages of nodularity are in between 83 and 89 % on average for the heats A and B, respectively. It can be concluded that the nodule count is decreased and the average nodule size is increased when the modulus is increased for both heats. It has been reported that the nodule count enhances and the nodule size decreases when the carbon equivalent increases [25]. In our case, the carbon equivalent was attained low and constant, and the distribution and features of graphite in the cast ductile iron produced were due to the nickel addition.

Figure 5 shows the etched microstructure of heats A and B for the casting modulus evaluated. It is observed for both heats, graphite nodules in a pearlitic-ferritic matrix, and in addition, heat A shows the presence of cementite.

Figure 6 shows the XRD pattern of the heats produced for the casting modulus evaluated. The presence of ferrite (JCPD file 00-006-0696) as the main phase in both heats and a small amount of cementite (JCPD file 00-035-0772) in heat A for the three casting modulus evaluated is observed. The phases identified match with those reported previously [24] in cast iron. The graphite phase (JCPD file 00-056-0159) has been reported [6] for a diffraction angle of 44 and 27°, the graphite phase is located very close to the (110) ferrite peak. A small graphite peak is observed at the diffraction angle of 44° for heat A and the casting modulus of 3.31 mm.

Figure 7 shows the presence of white regions identified as cementite only for heat A which was clearly revealed by the etching with ammonium persulfate with respect to the rest of the phases. It is evident that the amount of cementite is increased when the casting modulus is decreased.

Figure 8 shows results of scanning electron microscopy (SEM) and energy spectrum analysis (EDS) of heat B. It can be seen that the graphite nodule and nickel and silicon elements are distributed uniformly in the ferrite matrix, as was reported by Y. Sun [6].

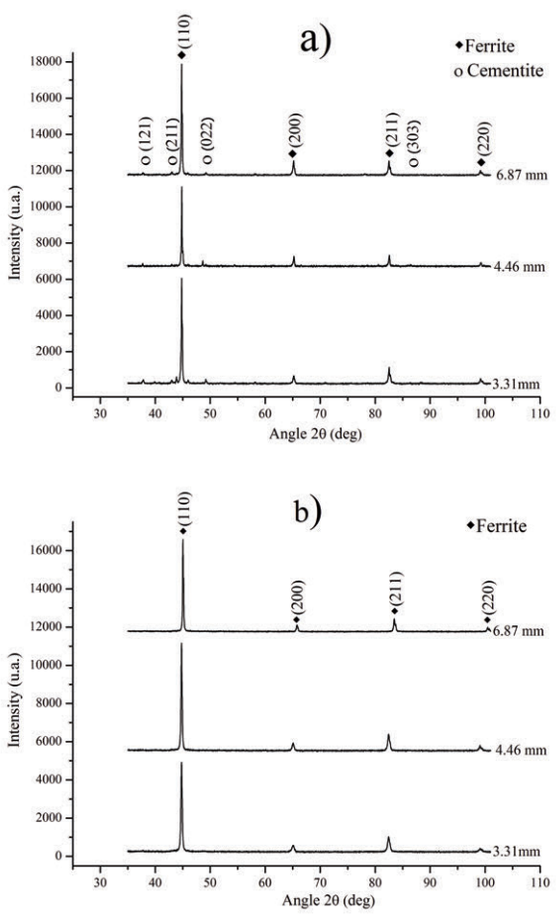

Figure 6. *X-ray pattern diffraction for casting modulus of 3.31, 4.46 and 6.87mm for a)HeatA and b)Heat B*

Table 3 shows the volume fraction of phases formed in both heats. The ferrite phase showed an increase in both heats when the casting modulus was increased while the pearlite phase showed an opposite behavior. Heat A shows a cementite formation for the three modulus evaluated.

Decreasing the thickness of casting increases the undercooling tendency and promotes metastable cementite eutectic formation. The carbon equivalent should be controlled to produce sound castings according to the section size. An equivalent carbon in the range of 4.3 to 4.6 for the section size lower than 51 mm is recommended [27]. R. Ruxanda [11] used high carbon equivalent (4.7) to avoid carbides formation in thin section castings with casting modulus of 1.1 and 2.1. In our case, for the hypo-eutectic chemical composition and the cooling rates imposed by the casting modulus evaluated, the

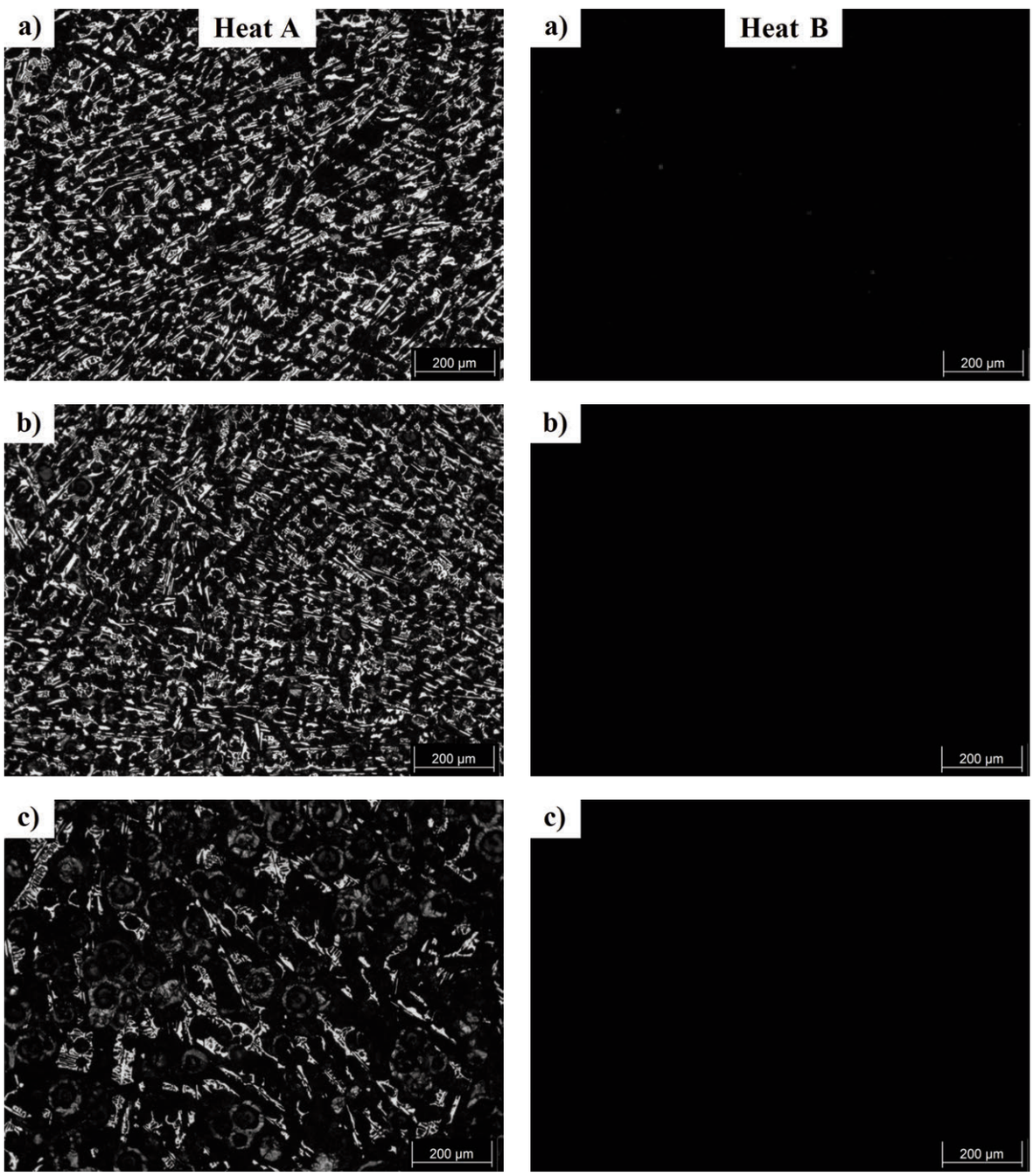

Figure 7. *Etched microstructure with ammonium persulfate reveals the cementite phase (white regions) of heats A and B for a casting modulus of a) 3.31 mm, b) 4.46 mm and c) 6.87 mm*

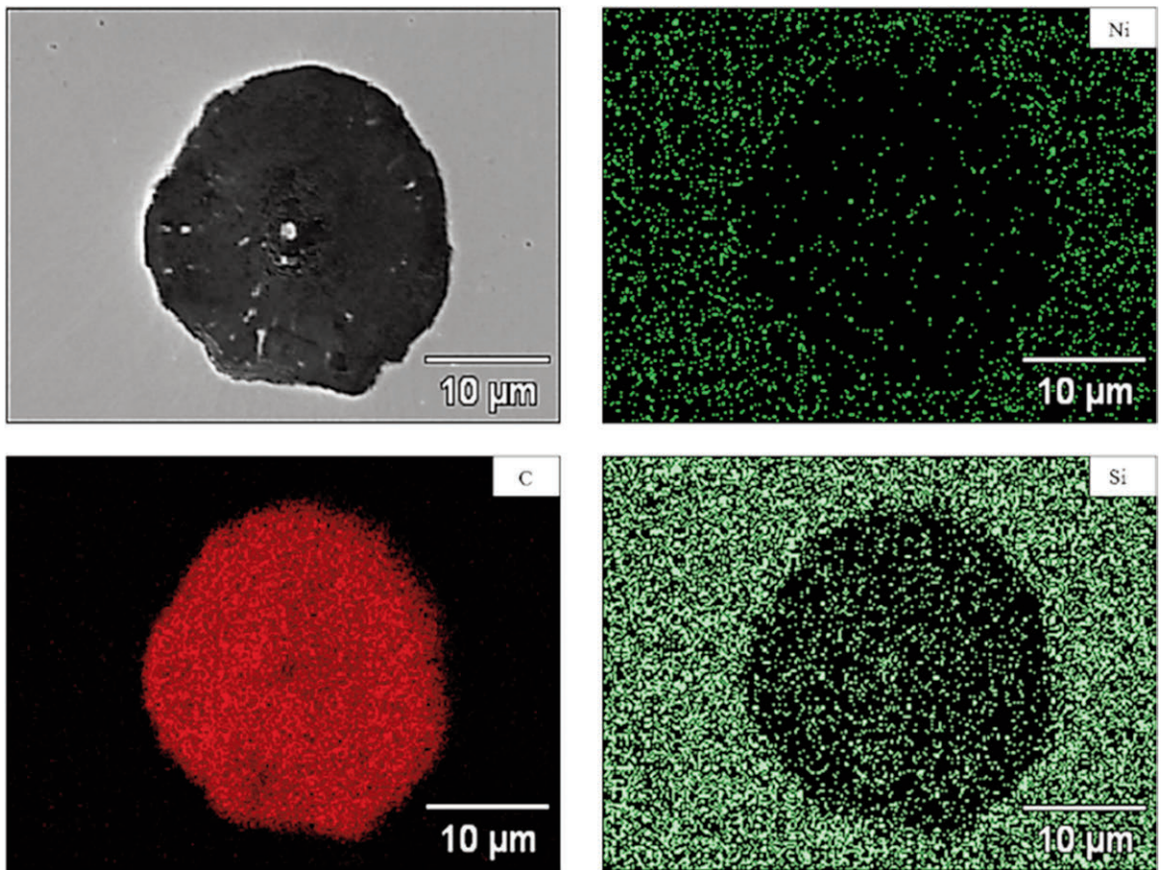

Figure 8. *Nodule image by SEM and X-ray mapping of nickel, carbon, and silicon*

Table 3. *Volume fraction of phases formed*

Casting modulus (mm)	Heat A			Heat B		
	3.31	4.46	6.87	3.31	4.46	6.87
Pearlite	65.93	61.04	52.98	71.40	69	62.7
Ferrite	5.20	9.97	23.02	11.39	17.54	25.1
Cementite	19.49	16.74	9.11	-	-	-
Graphite	9.37	12.24	14.87	17.21	13.46	12.2
Ferrite/Pearlite	0.07	0.16	0.43	0.15	0.25	0.40

cementite formation was unavoidable for heat A. In spite of the cementite formation, the chemical composition chosen gives good nodular graphite characteristics for the unalloyed ductile iron. The nickel addition in heat B avoids the cementite formation for the three casting modulus evaluated, as can be observed in Figure 7. It is observed that nickel is a pearlite former and allows to increase the nodule count. In addition, a higher nodule count indicates that there is a significant presence of ferrite in the matrix along with pearlite, as can be seen in the ratio ferrite/pearlite reported in Table 3. The ferrite/pearlite ratio is higher for heat B than heat A for the three modulus evaluated, which means an adequate balance between these two phases and the nodule count. The high nodule counts promoted by the nickel addition reduce inverse chill carbide formation associated with elemental segregation, besides higher homogeneity and a refined microstructure in the cast ductile irons, as can be observed in Figure 5 for heat B and the XRD patterns of figure 6b. Therefore, a high nodule count can reduce the likelihood of intercellular carbides. Nickel influences the structure of cast iron both as graphitiser and in its effect on the stability or decomposition of austenite. In the ternary Fe-C-Ni alloy, a beneficial effect of Ni on solidification is noted by the reduction of the carbon content of the eutectic. The interval between the γ-graphite and γ-Fe_3C eutectic transformation is increased. This latter influence is a factor in suppressing white iron formation [5]. The effect of the casting modulus on the Brinell hardness is shown in Figure 9 and Table 4.

Each point in figure 9 represents an average of six measurements in the central region of the plates in the longitudinal direction. The increase of the casting modulus decreases the Brinell hardness for both heats. Heat A shows the highest hardness values attributed to

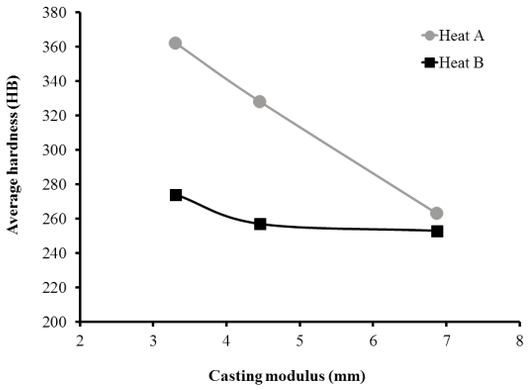

Figure 9. *Casting modulus effect on the average hardness for heats A and B*

Table 4. *Mechanical properties of the heats*

Casting modulus (mm)	Heat A			Heat B		
	3.31	4.46	6.87	3.31	4.46	6.87
Yield strength Ys (MPa)	460 ± 9.5	471 ± 9.2	537 ± 8.6	659 ± 7.2	480 ± 8.1	550 ± 6.1
Tensile strength Ts (MPa)	640 ± 8.9	643 ± 6.1	670 ± 7.2	734 ± 5.3	619 ± 7.9	620 ± 5.3
Ys/Ts	0.71	0.73	0.80	0.89	0.77	0.88
Brinell Hardness (HBN)	362 ± 3.4	328 ± 3.8	263 ± 3.1	274 ± 3.6	257 ± 4.3	253 ± 3.8

the pearlite amount and the cementite formation while heat B shows Brinell hardness values in the range from 253 to 274 for the casting modulus of 6.87 and 3.31 mm, respectively. Heat B promoted the highest ferrite amount for the casting modulus evaluated, despite the high level of pearlite promoted by the nickel addition (Table 3).

U. Seker et al [28] studied the effect of alloying elements on surface roughness and cutting forces during machining of ductile iron. The ductile iron samples were obtained from Y-II type casting block in accordance with ISO 1083. They report that the hardness increases when the nickel and copper additions were increased. The sample alloyed with 0.7 wt. % Ni reported a hardness of 23.68 HRC which correlate with the hardness reported in table 3, where the hardness value of 253 HBN (25 HRC) was obtained for the casting modulus of 6.87 for heat B. It has been reported [24] for low alloyed ductile iron that the hardness is increased due to the presence of alloying elements (Ni, Mo, and Cr) which in turn cause the formation of harder phases such as carbide and pearlite. The ferrite/pearlite ratio in the as-cast structure of heat B allows obtaining lower Brinell hardness values than heat A and a high nodule count in the casting modulus evaluated.

Tensile tests were carried out for three specimens of each casting modulus. Typical strain-stress curves were obtained. The average mechanical results and its standard deviation are shown in Table 4 for the casting modulus assessed. The variation of yield strength and tensile strength with the casting modulus is shown in Figure 8.

The unalloyed ductile iron (heat A) shows a slight increase in the tensile strength from 640 MPa to 670 MPa when the casting modulus is increased from 3.31 mm to 6.87 mm, respectively. This behavior is attributed to the smaller amount of cementite and pearlite for the casting modulus of 6.87 mm. Higher amounts of cementite and pearlite increase the hardness and decrease the tensile strength of the ductile iron, while the cast iron alloyed with nickel (heat B) shows that the tensile strength is decreased and remains almost constant when the casting modulus is increased from 4.46 to 6.87 mm due to the similar amounts of pearlite in both casting modulus. The highest tensile strength value (734 MPa) was obtained for heat B with the casting modulus of 3.31 mm. This behavior is attributed to the presence of the highest amounts of pearlite and nodule count, as can be observed in Tables 2 and 3, respectively. E. Konca et al [29] reported hardness and tensile strength values of 236 HBN and 677 Mpa for a ductile cast iron alloyed with 0.4 wt % Ni in the as-cast condition, which is into the range expected based on the results reported in table 4.

Nickel as a solute element dissolved in the matrix (Figure 8), interacts with the dislocations and the elements segregated around dislocations increasing their motion resistance by forming Cottrell atmosphere [20]. But, when nickel exceeds 0.8 wt. %, the existence of increasing solute element strengthens the dislocation motion resistance and pining constant which reflects an increase of the tensile strength and a decrease of the impact energy of the ductile iron [6]

The tensile strength values for both heats showed a similar behavior for the three modulus evaluate; however; the tensile strength (T_s)- yield strength (Y_s) ratio reported in Table 4 shows that the gap between both strengths becomes higher and more constant in 0.84 against 0.74 in average for heats B and A, respectively. The (Y_s/T_s) ratio may indicate a more homogeneous behavior on the yield and tensile strength and could be related to the smooth trend obtained in the nodule count and the average nodule size behavior for the ductile iron alloyed with nickel and the casting modulus evaluated.

The results show that nickel addition to the ductile iron increases the nodule count as the solidification rate increases when the casting modulus decreases.

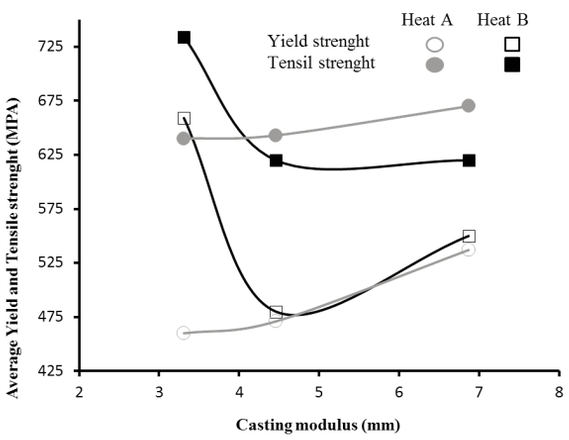

Figure 10. *Casting modulus effect on the average yield and tensile strength for heats A and B*

The nickel as a graphitizing element reduces the solubility of carbon in liquid iron, increasing the carbon interaction with the reactive elements of the inoculant, and providing effective heterogeneous nucleation sites as rapid solidification proceeds when the casting modulus is decreased. A decrease of the diffusion distances for the migration of carbon from the matrix to the nodules and vice-versa occurs when the nodule count is increased [30]. For these conditions, a higher amount of graphite is obtained, as well as a high nodule count. When the casting modulus is increased, the nodule count decreases and the graphite grows with the carbon diffusion to graphite nodule through the austenite layer during the eutectic solidification increasing the nodule size. However, when the casting modulus decreases for the unalloyed ductile iron (heat A), the undercooling tendency increases and promotes metastable cementite eutectic formation. Therefore a more effective inoculant must be used to avoid cementite formation in order to increase the spheroidal graphite in thin wall castings.

4. Conclusions

The effect of the casting modulus on the distribution and features of graphite in cast ductile iron unalloyed and alloyed with 0.88 wt. % nickel has been studied. The results obtained can be summarized as follows:

1. The decrease of the casting modulus from 6.87 mm to 3.31 mm increases the nodule count from 127 to 357 nod mm-2 and from 290 to 606 nod mm^{-2}, for the ductile iron unalloyed and alloyed with nickel, respectively.

2. The increase of the casting modulus increased the nodule size and decreased the nodule count for both heats; however, for heat B, the nodule size increased slightly and homogeneous than heat A, showing a high nodule count with adequate size and distribution.

3. The decrease of the casting modulus increased the undercooling tendency and promoted the cementite formation in heat A, this behavior was suppressed by the nickel addition in heat B for the casting modulus evaluated.

4. The nickel addition improves the efficiency of the conventional inoculant used by reducing the solubility of carbon in liquid iron, increasing the carbon interaction with the reactive elements of the inoculant, providing effective heterogeneous nucleation sites when the casting modulus is decreased.

5. The nickel addition in heat B promoted the highest ferrite/pearlite ratio regarding heat A that improve the nodule count and spherical graphite for the casting modulus evaluated.

6. The yield and tensile strengths were found to keep almost constant (Y_S/T_S = 0.84 in average) for heat B which could mean a homogenous mechanical behavior for the casting modulus evaluated.

Acknowledgments

The authors wish to thank the Institutions CONACyT, SNI, COFAA and SIP-Instituto Politécnico Nacional for their permanent assistance to the Process Metallurgy Group at ESIQIE-Metallurgy and Materials Department.

References

[1] M. Perzyk, A. W. Kochanski, J. Mater. Process. Technol., 109 (2001) 305-307.

[2] A. Kujawińska, M. Rogalewicz, M. Diering, M. Piłacińska, A. Hamrol, A. Kochański, J. Min. Metall. Sect. B-Metall., 52 (1) (2016) 25 – 34.

[3] R. E. Ruxanda, D. M. Stefanescu, T. S. Piwonka, AFS Transactions, 02-177 (2002) 1-17.

[4] Ch. F. Han, Y. F. Sun, Y. Wu, Y. H. Ma, Metallogr. Microstructure., Anal 4 (2015) 135-145.

[5] I. Minkoff, Alloy Cast Iron systems, The Physical Metallurgy of Cast Iron. John Wiley and Sons Ltd., Norwich, England, 1983, p. 185-188.

[6] S. Yufu, Hu Sumeng, X. Zhiyun, Y. Sansan, Z. Jingyu, L. Yezhe, Materials and Design, 41 (2012) 37-42.

[7] W. F. Smith, Cast Irons, Structure and Properties of Engineering Alloys, Mc Graw-Hill Inc., USA, 1981, p. 333-343.

[8] R. Gonzaga, J. Carrasquilla, J. of Mater. Process. Technol., 162-163 (2005) 293-297.

[9] J. Keough, K. Hayrynen, G. L. Pioszak, AFS Proceedings. Schaumburg. IL USA. Paper 10 (2010) 1-15.

[10] R. Källbom, K. Hamberg, M. Wessén, L. Björkegren, Mater. Sci. Eng. A, 413-414 (2005) 346-351.

[11] R. Ruxanda, L. Beltran, J. Massone, D. Stefanescu, AFS Transactions, 109 (2001)1037-1047.

[12] L. Achour, M. Martínez, R. Boeri, J. Sikora, Proceedings of the SAM 2000 Congress, August, Neuquén, Argentina, 2000, p.115-122.

[13] G. Cooper, A. Roebuck, H. Bayati, R. Elliot, Int. J. Cast Met. Res., 11(1999) 227-235.

[14] J. Massone, R. Boeri, J. Sikora, Int. J. Cast Met. Res., 16, 1-3 (2003) 251-256.

[15] N. Rebasa, R. Dommarco, J. Sikora, Wear, 253 (2002) 855-861.

[16] R. Dommarco, A. Jaureguiberry, J. Sikora, Wear, 261 (2006) 172-179.

[17] R. Martínez, R. Boeri, J. Sikora, Proceedings of the 2002 World Conference on ADI AFS Publication, September 26-27, Louisville, Kentucky USA, 2000, p. 143-148.

[18] S. Lekakh, Jr. Loper, C.R., AFS Transactions, (2003)1-10.

[19] I. Lee, Proceedings of the 2002 World Conference on ADI AFS Publication, AFS Publication, September 26-27, Louisville, Kentucky USA, 2002, p. 7-13.

[20] P. Sellamuthu, D.G. Harris, D. Dinakaran, V. P. Premkumar, Li Zushu, S. Seetharam, CMSME 2018 IOP Conf. Series: Materials Science and Engineering, February 24-26, Bangkok, Thailand, 2018, 1-7.

[21] D. Pedro, R. Dommarco, Wear, 418-419 (2019) 94-101.

[22] G. Rivera, R. Boeri, J. Sikora, Adv. Mater. Res., 4-5 (1997) 169-174.

[23] N. Fatahalla, H. Hakim, A. El-Ezz, M. Mohamed, J. Mat. Sci., 31 (1996) 4933-4937.

[24] A. Refaey, N. Fatahalla, J. Mat. Sci., 38 (2003) 351-362.

[25] N. Fatahalla, H. Hakim, A. Ezz, M. Mohamed, J. Mat. Sci., 31, 49 (1996) 93-4937.

[26] L. Battezzanti, M. Baricco, S. Curiotto, Acta Materialia., 53 (2005) 1849-1856.

[27] K. Hayrynen, Proceedings of the 2002 World Conference on ADI AFS Publication, September 26-27, Louisville, Kentucky USA, 2000, p. 1-6.

[28] U. Seker, I. Ciftci, H. Hasirci, Materials and Design, 24 (2003) 47-51.

[29] Erkan Konca, Kazım Tur, Erkin Koç, Metals, 7 (2017) 320.

[30] J. M. Massone, R. E. Boeri, J. A. Sikora, Int. J. Cast Met. Res., 16, 1-3 (2003) 179-184.

UTICAJ DODAVANJA NIKLA I MODULA ZA LIVENJE NA OSOBINE HIPO-EUTEKTIČKOG NODULARNOG LIVENOG GVOŽĐA

E. Colin-García [a], A. Cruz-Ramírez [a*], G. Reyes-Castellanos [a], J.A. Romero-Serrano [a], R.G. Sánchez-Alvarado [a], M. Hernández-Chávez [b]

[a*] Nacionalni politehnički institut – ESIQIE, Odsek za inženjerstvo metalurgije i materijala, Meksiko Siti, Meksiko

[b] Nacionalni politehnički institut – UPIIH, Odsek bazičnih nauka, Pachuca, México

Apstrakt

Proučavan je uticaj modula za livenje na distribuciju i osobine grafita u hipo-eutektičnom gvožđu koje je nelegirano i koje je legirano niklom (0.88 wt %). Stopa hlađenja ploča za livenje debljine 25.4, 12.7 i 8.5 mm sa modulima za livenje od 6.87, 4.46 i 3.31 mm dovodi do nekoliko mikrostrukturnih promena, kao što su precipitacija cementita i primetno povećanje broja nodula. Dodavanje nikla je suzbijalo formiranje cementita i povećavalo broj nodula i nodularnost tri procenjivana modula livenja. Dodavanje nikla povećava broj nodula 69, 67 i 128 % za module od 3.31, 4.46 i 6.87 mm što se tiče nelegiranog nodularnog gvožđa. Otkriveno je da najveći moduli livenja proizvode najveće nodule uz najniži broj nodula kod obe vrste nodularnog livenog gvožđa. Poboljšanjem osobina grafita, dodavanje nikla omogućava da se odnos razvlačenja i vlačne čvrstoće održava gotovo konstantnim za različite module livenja.

Ključne reči: *Nodularno gvožđe; Broj nodula; Nikl; Moduli livenja; Mehaničke osobine.*